

Selected Test Results of Railway Ballast in Terms of Heavy Axle Loads for Bearing Capacity Calculations

Anastasia KONON^{a,1}

^a*Emperor Alexander I St. Petersburg State Transport University*

Abstract. This paper presents the results of field and laboratory tests of railway ballast. Field tests were aimed to study the vibrational acceleration of ballast particles and ballast layer stressed state in terms of train traffic with heavy axle loads. The test results are vibrational acceleration and stress values distribution in ballast layer and experimental relationships of vertical and horizontal vibroaccelerations damping in terms of train operation with axle load up to 300 kN. Laboratory stabilometer tests were directed to study the change of ballast strength properties due to vibrodynamic impact and shows that for dynamic loading with 10, 25, 55 Hz frequencies vibrodynamic impact influences strength properties insignificantly and coincides with the accuracy of test equipment. Stated test results provide references for calculation of ballast and sub-ballast bearing capacity.

Keywords. Ballast, vibrational acceleration, vertical stress, heavy axle load, stabilometer.

1. Introduction

An important developmental area for Russian railway transport is increasing car axle load. Nowadays JSC «Russian Railways» possesses cars with 230 kN axle load. They amount 88% from a total of 1 million freight cars. Cars with 230 kN axle load are gradually replaced with new ones with 250 kN axle load. Research and production corporation «United Wagon Company» has developed new cars with 270 kN axle load in 2017.

Thus, the task of track stable performance under increasing train dynamic load is vitally important. Worldwide operating experience and in-situ tests [1] show that increasing axle load standards and train speed induce growth in the number of defects in ballast, subballast and subgrade [2].

Railway track stability depends not only on subgrade sustainability and quality of ties, fastenings and rails but also on the quality of all subballast elements and the ballast itself. The main cause of ballast reliable performance is its bearing capacity which depends on the level of vibrational dynamic load applied to the ballast layer [3], subballast and subgrade characteristics. Ballast layer bearing capacity and deformability depend on ballast friction angle, moduli of deformation and elasticity. These

¹ Corresponding Author, Anastasia Konon, Construction of Roads for Transportation Complex Department, Emperor Alexander I St. Petersburg State Transport University, Moskovskiy pr. 9, St. Petersburg, 190031, Russia. E-mail: a.a.konon@mail.ru.

characteristics depend on a number of factors such as vibrational dynamic load level under the sleeper pad, ballast gradation, fouling, density, roundness, subsleeper damper presence and its stiffness. Values of these characteristics and their change according to tonnage accumulation allow prediction of ballast bearing capacity, deformability and overhaul life. However, little attention has been paid to ballast strength and deformative properties and their change according to tonnage accumulation in terms of vibrational dynamic load. Indirect methods of defining ballast strength and deformative properties are quite ungrounded, often uncertain and may provide inaccurate calculation results.

2. Materials and methods

Emperor Alexander I St. Petersburg State Transport University (PGUPS) scientists held in-situ tests of vertical vibrational accelerations of ballast particles and ballast layer stressed state. These tests were held at the Russian Railway Research Institute experimental track. The on-site rolling stock had axle loads of 230 to 300 kN at a speed of 70 km/h.

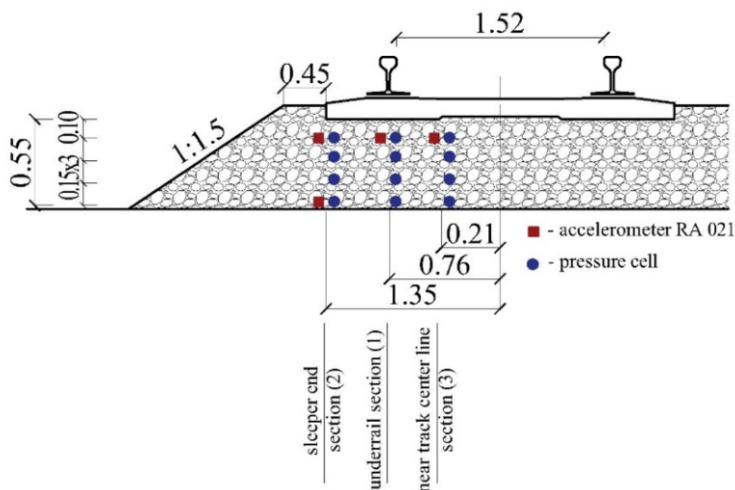


Figure 1. Sensor placement in the ballast layer and subballast (all measurements in metres).

Track structure had the following parameters: 65 kg/m rails, concrete sleepers (2,000 items/km), tension clamp fastenings ARS-4, and thickness of granite ballast was 55 cm under the sleeper. Ballast consisted of 25–60 mm particles. Vertical vibrational accelerations were measured with RA 021 accelerometers. These sensors provide measurements of acceleration up to 200 m/s² and frequency of 5–5,000 Hz. Accelerometers were connected to seismic station ZET 048. Vertical stress values in the ballast layer were measured with soil pressure capsule set. Sensors were placed under the sleeper and in the depth of ballast layer. Sensors were set at the sleeper end, underrail section, and near the centre line of the track and up to 55 cm under the sleeper (at the sleeper end). Sensor placement in the ballast layer and subballast is presented in Figure 1.

Laboratory tests involved unconsolidated-undrained triaxial compression tests, held in a vacuum apparatus (Figure 2). Tests were directed to study the change of ballast strength properties due to vibrational dynamic impact. The test specimen diameter was

265 mm and height ~ 530 mm. Specimens were made of granite and gabbro-diabase crushed stone with a gradation range of 25–60 mm. Tests were made in terms of static and dynamic loading with lateral pressure 80 and 130 kPa and frequencies of 10, 25 and 55 Hz. Test data included lateral and failure stresses used determination of strength properties with Mohr's circles.

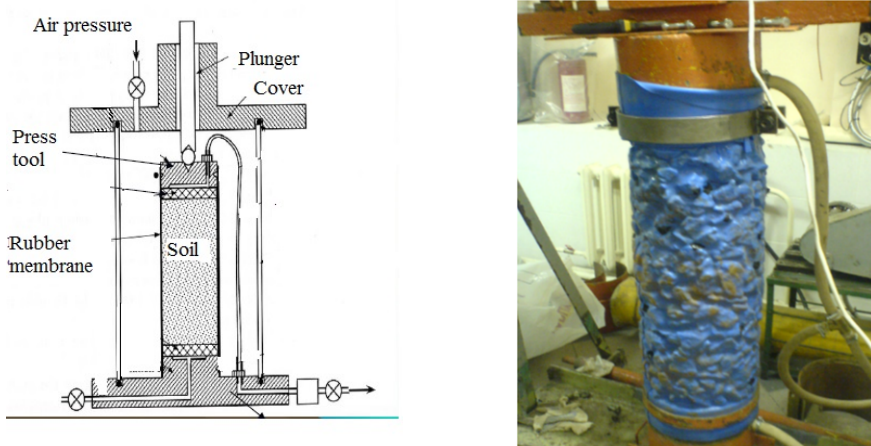


Figure 2. Triaxial apparatus setup (left). Crushed stone unconsolidated-undrained triaxial compression tests (right).

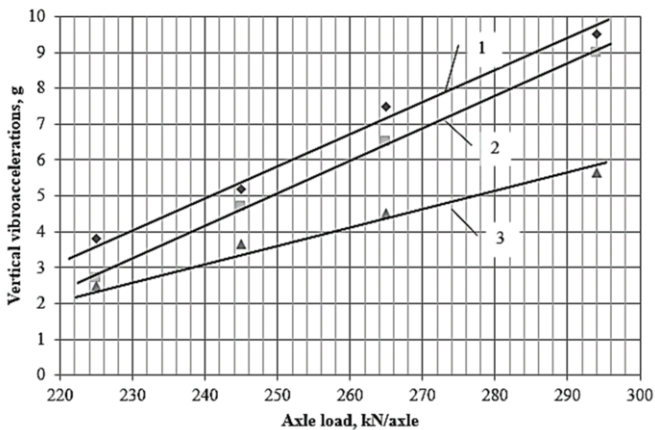


Figure 3. Vertical vibrational acceleration distribution at the level of 10 cm under the sleeper: 1 – at underrail section, 2 – at the sleeper end, 3 – near center line of a track.

3. Analysis of test results

Test results show that axle load increasing causes the rise of vibrational acceleration and stress values in ballast and subballast. Vertical vibrational acceleration and stress distribution charts at levels of 10 and 55 cm under the sleeper are presented in Figures 3 - 6.

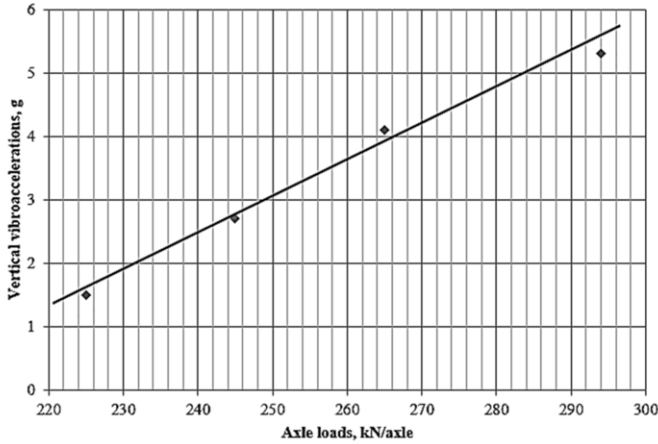


Figure 4. Vertical vibrational acceleration distribution at the level of 55 cm at the sleeper end.

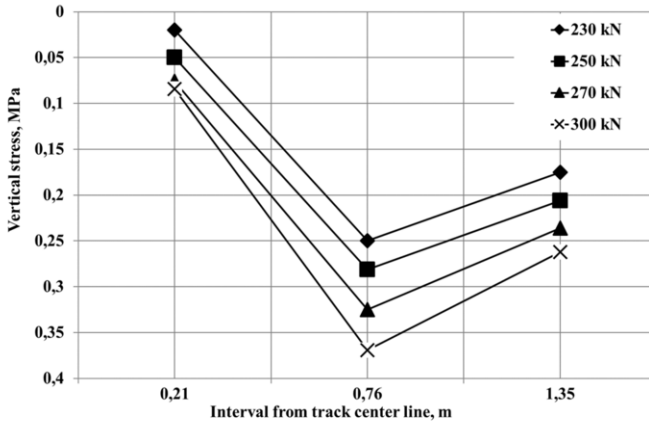


Figure 5. Vertical stress distribution at the level of 10 cm under the sleeper pad with axle loads: 1 – 230, 2 – 250, 3 – 270, 4 – 300 kN.

Analysis of test data shows that increasing of rolling stock axle load from 225 to 300 kN causes the growth of vertical vibrational accelerations. Maximal values of accelerations are recorded at the underrail section, reaching from 3.8 to 9.5g and growing 2.5x. At the sleeper end, vertical accelerations are about 15% lower than at the underrail section, with amounts of 2.7 to 9g for 225–300 kN axle load at a depth of 10 cm under the sleeper pad. The lowest values are near the track centre line, which change from 2.5 to 5.7g. Statistical analysis of test data provides an experimental relationship of vertical vibrational acceleration damping [4-6] in terms of train operation with axle load up to 300 kN:

$$\frac{d^2U}{dt^2} = g_0^v \exp(-\delta_z^v z - -\delta_y^v y) \tag{1}$$

where: g_0^v is vertical vibroacceleration under the sleeper pad; δ_z^v is vertical vibroacceleration damping factor in the vertical plane; δ_y^v is vertical vibroacceleration

damping factor in the horizontal plane; z , y are point coordinates. Test results show that the axle load increase causes a rise of stress values in ballast and subballast. Vertical stress distribution charts at levels of 10 and 55 cm under the sleeper pad are presented in Figures 5 and 6.

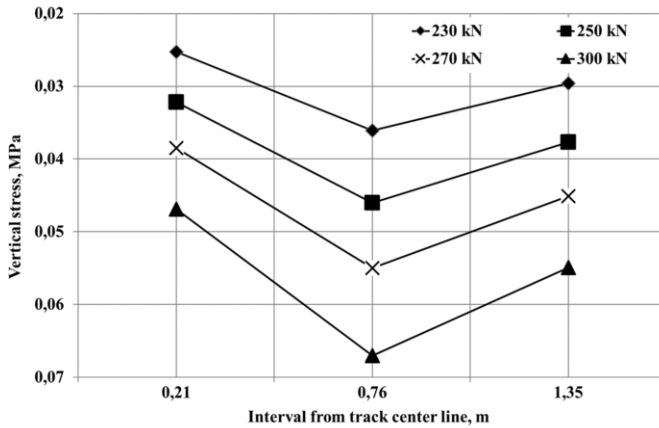


Figure 6. Vertical stress distribution at the level of 55 cm under the sleeper pad with axle load: 1 – 230, 2 – 250, 3 – 270, 4 – 300 kN.

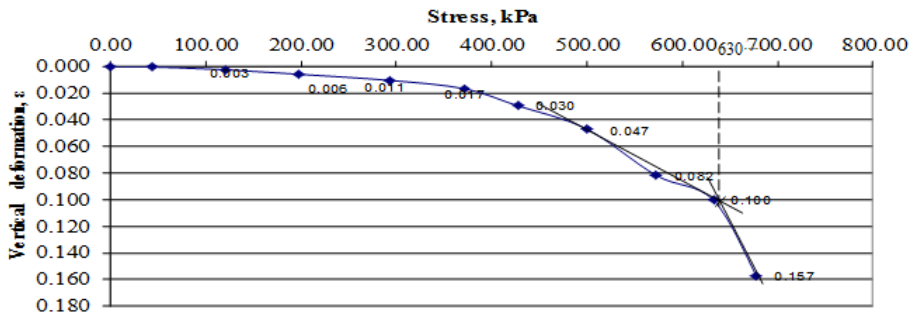


Figure 7. Example of stress-strain curve for granite crushed stone for lateral pressure 130 kPa.

Data analysis from Figures 5 and 6 shows that the car axle load primarily affects ballast and subballast stressed state. Vertical stress under the sleeper pad and ballast layer grow intensively as a result of increasing axle load. Thus, at the underrail section at the level of 10 cm under the sleeper pad stress became 1.5 times as much and at the level of 55 cm under the sleeper pad, they increased 1.9 times due to axle load change from 230 to 300 kN. This stressed state change should be taken into account while designing the ballast layer and subballast structure from the point of bearing capacity. Derived stress values are used as operating stress values in ballast and subballast strength inequality (or condition) [4, 5] (Eq. (2)):

$$\sigma_z \leq \frac{[\sigma_z]}{\gamma_n} \tag{2}$$

where: σ_z is operating stress value; $[\sigma_z]$ is limit stress value according to ballast bearing capacity calculation, and γ_n is the reliability factor.

As a result of laboratory tests, crushed stone strength properties were determined with Mohr's circles. Circles plotting is based on crushed stone stress-strain curves obtained in tests and critical stress. An example of a stress-strain curve and determining of critical stress is presented in Figure 7.

Mohr's circles were plotted considering the statistical analysis of critical stresses obtained in similar conditions for similar type and quality of specimen material (Figures 8–11).

Test data shows that for dynamic loading with 10, 25, 55 Hz frequencies vibrational dynamic impact influences strength properties insignificantly and coincides with an accuracy of test equipment. The angle of internal friction reduction under vibrational dynamic loading reached 5% for granite crushed stone and 7% for gabbro-diabase. These results are used in ballast bearing capacity calculations for decreasing ballast strength properties to model the vibrational dynamic impact [4, 5].

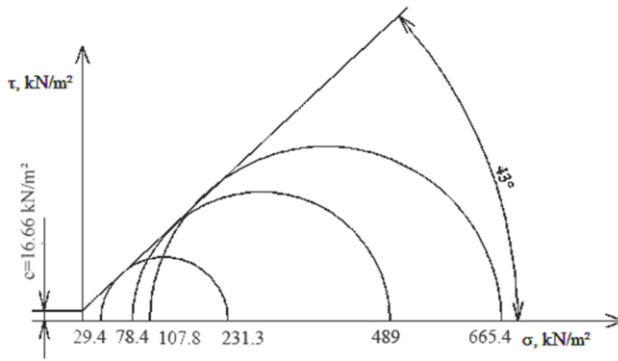


Figure 8. Strength properties determination of granite crushed stone in terms of static loading.

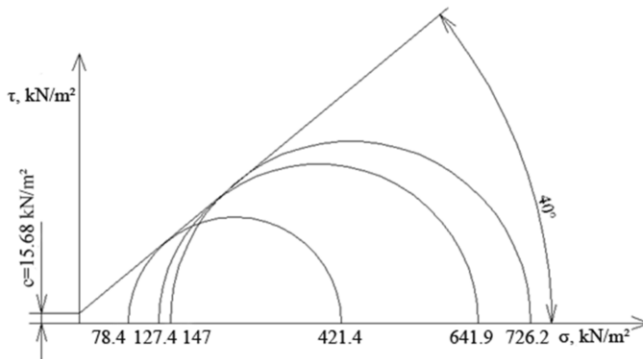


Figure 9. Strength properties determination of granite crushed stone in terms of dynamic loading.

4. Practical problems

Obtained data and analysis results are used in calculations of ballast bearing capacity, based on ballast and subballast limiting equilibrium state [4, 5].

Using laboratory tests results and the stated mathematical model, bearing capacity dependence on the operating parameters can be derived, such as accumulated tonnage, speed, and axle load. This complex research will help solve scientific and practical problems of ballast bearing capacity, deformability and overhaul life and optimize track reliability costs.

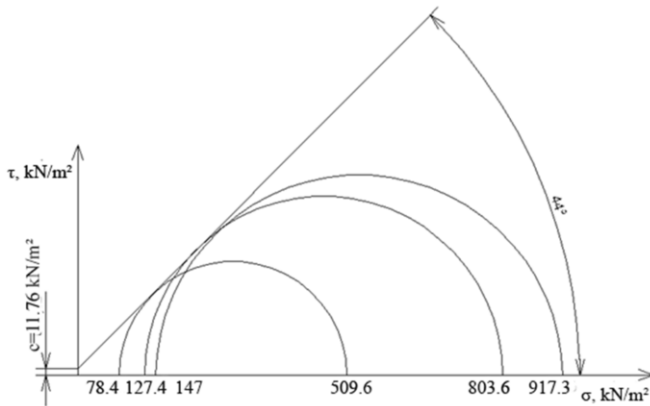


Figure 10. Strength properties determination of gabbro-diabase crushed stone in terms of static loading.

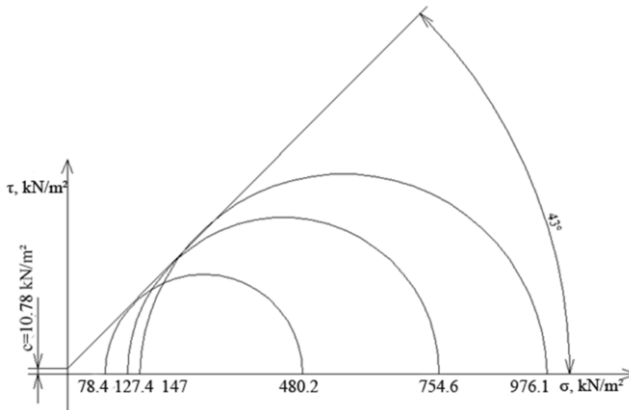


Figure 11. Strength properties determination of gabbro-diabase crushed stone in terms of dynamic loading.

5. Conclusions

Field test data shows that increasing of rolling stock axle loads from 225 to 294 kN/axle causes the growth of vertical vibrational acceleration and stress. Maximal values are recorded in the underrail section. At the sleeper end, vertical accelerations are about 15% lower. Experimental relationship of vertical vibrational acceleration damping in terms of train operation with axle load up to 300 kN was derived (Eq. (1)). Vertical stress under the sleeper pad and ballast layer grow intensively as a result of increasing axle load. Thus, at the underrail section (Figures 4, 5) at the level of 10 cm under the sleeper pad, stress

became 1.5 times as much and at the level of 55 cm under the sleeper, they increased 1.9 times.

Laboratory tests of crushed stone strength properties show that vibrational dynamic impact influences strength properties insignificantly and coincides with the accuracy of test equipment. The angle of internal friction reduction under vibrational dynamic loading reached 5% for granite crushed stone and 7% for gabbro-dabase. These results are used in ballast bearing capacity calculations for decreasing ballast strength properties to model the vibrational dynamic impact.

References

- [1] Petriaev A., The vibration impact of heavy freight train on the roadbed, *Procedia Engineering* **143** (2016), 1136-1142.
- [2] Petriaev A., Stress Response Analyses of Ballasted Rail Tracks, Reinforced by Geosynthetics, *Procedia Engineering* **189** (2017), 660-665.
- [3] Tutulumluer E., Qian Y., Hashash Y.Y.M.A., Ghaboussi J., Field validated discrete element model for railroad ballast, *Proceedings of the American Railway Engineering and Maintenance-of-Way Association Annual Conference* (2011) https://www.arena.org/proceedings/proceedings_2011.aspx
- [4] Kolos A., Konon A., Estimation of railway ballast and subballast bearing capacity in terms of 300 kN axle load train operation, *Challenges and Innovations in Geotechnics. Proc. intern. conf., Astana, 5-7 August* (2016).
- [5] Kolos A., Konon A., Darienko I., Mathematical Model for Forecasting of Rail Track Ballast Bearing Capacity, *Procedia Engineering* **189** (2017), 916-923.
- [6] Konon A., Vibrational acceleration distribution in railway ballast in terms of heavy axle load operation, *5th International Conference on Road and Rail Infrastructure, Zadar, Croatia, Tiskara Zelina, 2018, 1209-1213.*
- [7] Petriaev A., Konon A., Influence of geosynthetics on the oscillations amplitude of railway subgrade, *Proceedings of 11th ICG, Seoul, Korea, 2018.*